

Copyright 1999 Society of Photo-Optical Instrumentation Engineers.

This paper was published in the SPIE Proceeding, Imaging Spectrometry V, Volume 3753, July 1999 and is made available as an electronic reprint with permission of SPIE. Single print or electronic copies for personal use only are allowed. Systematic or multiple reproduction, or distribution to multiple locations through an electronic listserver or other electronic means, or duplication of any material in this paper for a fee or for commercial purposes is prohibited. By choosing to view or print this document, you agree to all the provisions to the copyright law protecting it.

Atmospheric Correction for Short-wave Spectral Imagery Based on MODTRAN4

S.M. Adler-Golden^{*a}, M.W. Matthew^a, L.S. Bernstein^a, R.Y. Levine^a, A. Berk^a, S.C. Richtsmeier^a, P.K. Acharya^a, G.P. Anderson^b, G. Felde^b, J. Gardner^b, M. Hoke^b, L.S. Jeong^b, B. Pukall^b, J. Mello^b, A. Ratkowski^b and H.-H. Burke^c

^aSpectral Sciences, Inc., 99 South Bedford St., Burlington, MA 01803

^bAir Force Research Laboratory, Space Vehicles Directorate, Hanscom AFB, MA 01731

^cMIT Lincoln Laboratory, Lexington, MA 02173

ABSTRACT

A new, state-of-the-art atmospheric correction algorithm for the solar spectral range has been developed based on the MODTRAN4 code. The primary data products are surface reflectance spectra, column water vapor maps and relative surface elevation maps. In addition, a radiance simulation tool, an automated visibility retrieval algorithm and a spectral "polishing" algorithm are included. Validations of retrievals have been carried out by analyzing data that encompass a variety of atmospheric and surface conditions. Some results and their implications for atmospheric correction and spectroscopy are discussed.

Keywords: MODTRAN, AVIRIS, atmospheric, correction, compensation, spectral, retrieval, algorithm, reflectance

1. INTRODUCTION

Remotely sensed spectral imagery of the Earth's surface can be used to fullest advantage only when the influence of the atmosphere has been removed and the data are reduced to units of reflectance. Recently, we have initiated the development of a new, state-of-the-art atmospheric "correction" or "compensation" algorithm for spectral imaging sensors. This algorithm utilizes MODTRAN4, the latest version of the well-known MODTRAN radiative transfer code developed by Spectral Sciences, Inc. (SSI) and the Air Force Research Laboratory (AFRL), which is now available through AFRL.¹ The algorithm automates the MODTRAN4 radiance calculations used to construct the look-up tables (LUTs) needed for solving the retrieval (inverse) problem. In addition, operation in a forward mode allows the generation of high-fidelity synthetic radiance data cubes for arbitrary atmospheric and viewing conditions starting from surface reflectances.

Recent efforts have focused on validating the algorithm using ground-truth data, adding new capabilities and improving user friendliness. An important part of validating the atmospheric correction procedure and MODTRAN4 itself has been the analysis of imagery taken under less than optimal atmospheric conditions, including low visibility, high moisture and low sun. These cases are especially stressing and have helped identify some areas of weakness in the molecular spectroscopic models.

2. METHODOLOGY

The standard equation for spectral radiance L^* at a sensor pixel is^{2,3,4}

$$L^* = A\rho/(1-\rho_e S) + B\rho_e/(1-\rho_e S) + L^*_a \quad (1)$$

which applies for SWIR through UV wavelengths, where thermal emission is negligible. Here ρ is the pixel surface reflectance, ρ_e is an average surface reflectance for the pixel and the surrounding region, S is the spherical albedo of the atmosphere, L^*_a is the radiance backscattered by the atmosphere and A and B are coefficients that depend on atmospheric and geometric conditions. The first term in Equation (1) corresponds to the radiance from the surface that travels directly into the sensor, while the second term corresponds to the radiance from the surface that is scattered by the atmosphere into

*Correspondence: Email: sag@spectral.com; WWW: <http://www.spectral.com>; Telephone: 781 273 4770; Fax: 781 270 1161

the sensor. The distinction between ρ and ρ_e accounts for the "adjacency effect" (spatial mixing of radiance among nearby pixels) caused by atmospheric scattering. The adjacency effect correction may be turned off by setting $\rho_e = \rho$.

For a specified model atmosphere the values of A, B, S and L_a^* in Equation (1) can be determined empirically from the standard MODTRAN4 outputs of total and direct-from-the-ground spectral radiances computed at three different surface reflectance values, such as 0, 0.5 and 1. The viewing and solar angles of the measurement and nominal values for the surface elevation, aerosol type and visible range for the scene are used. To account for possible variations in column water vapor across the scene these calculations are looped over a series of varying water profiles. This step is facilitated by a new feature in MODTRAN4 which allows a scale factor to be applied to the nominal water profile of the model atmosphere.

As in other atmospheric correction codes,^{5,6} before the data are converted to reflectance the column water vapor is retrieved on a pixel-by-pixel basis. This is done using radiance averages for two sets of channels, an "absorption" set centered at a water band (typically the 1.13 μm band) and a "reference" set of channels taken from the edge of the band. The water retrieval is performed rapidly with a 2-dimensional look-up table (LUT) constructed from the MODTRAN4 outputs using a-Delaunay triangulation procedure. One dimension of the table is the "reference" to "absorption" ratio and the other is the "reference" radiance. The second dimension accounts for a reflectance-dependent variation in the ratio arising from the different amounts of absorption in the atmospherically-scattered and surface-reflected radiance components; the absorption is generally smaller for the atmospherically scattered photons because they avoid the high concentration of water vapor close to the ground.

After the water retrieval is performed, Equation (1) is solved for the pixel surface reflectances in all of the sensor channels. The solution is based on a method, described by several authors,^{3,6} in which a spatially averaged radiance image is used to generate a good approximation to the averaged reflectance ρ_e . The averaging is performed using a point-spread function that describes the relative contributions to the pixel radiance from points on the ground at different distances from the direct line of sight. Presently this function is taken as a wavelength-independent radial exponential; its width is determined from a single-scattering calculation that accounts for the sensor altitude, the aerosol scale height and a nominal aerosol phase function (Henyeey-Greenstein with asymmetry parameter = 0.7). We anticipate implementing in the future a more rigorous approach that accounts for spectral dependencies and the different scale height and phase function that apply to Rayleigh scattering.

A procedure analogous to the water vapor determination can be used to retrieve a scene elevation map. Here the MODTRAN4 calculations are looped over elevation rather than water vapor concentrations and an absorption band of a uniformly mixed gas such as O_2 or CO_2 is interrogated. Reasonable relative (and in some cases absolute) elevations have been obtained from AVIRIS images using either the 762 nm O_2 band or the 2.06 μm CO_2 band.

MODTRAN4 options can be selected that control the tradeoff between accuracy and computational speed. These include the number of water vapor column amounts, the multiple scattering algorithm (Isaacs 2-stream or DISORT n -stream), band model resolution (standard 1 cm^{-1} or fast 15 cm^{-1}) and radiative transport algorithm (standard band model with Curtis-Godson path averaging or correlated- k). There are also several different choices of the solar irradiance function. While full MODTRAN accuracy requires 16-stream DISORT, 1 cm^{-1} resolution and the correlated- k algorithm, good results are obtained with the Isaacs and standard band model algorithms with acceptable computation times (around 1 hour on a 300 MHz PC). The 15 cm^{-1} band model parameters are a new feature of MODTRAN4 and have been optimized to approach the accuracy of a resolution-degraded 1 cm^{-1} calculation.

3. AEROSOL RETRIEVAL

Atmospheric aerosol impacts not only the quantity of backscatter but also the attenuation of the surface-reflected radiance and the magnitude of the adjacency effect. Typically, "guesstimates" are made for the aerosol type and amount (i.e., as given by the optical depth or visible range); these may be refined, as desired, through iterative comparisons of reflectance retrievals against "known" surfaces. This iterative process is tedious and time-consuming, however. Recently we have developed several methods for single-step retrieval of the visible range, which is inversely related to the aerosol amount, from the scene information. This aerosol retrieval is most conveniently performed as the first step in the atmospheric correction process (prior to the water vapor determination).

One method assumes that the surface reflectance at one or a set of adjacent wavelength channels is known for one or more "reference" pixels. Best results are obtained using visible wavelengths and either a very dark surface, such as vegetation or deep calm water, or a very bright surface, such as a white calibration target that is large enough to fill at least one pixel. The sensor's absolute radiance calibration must be very accurate in the latter case, where the main aerosol effect is attenuation rather than backscattering. The method operates as follows. MODTRAN4 calculations over a bandpass containing the selected sensor channel(s) are performed for a series of visible range values, e.g. 200., 100., 50., 33., 25., 20. and 16.7 km, that are evenly spaced in their reciprocals (optical depths). The water vapor profile chosen is unimportant as long as there is negligible water absorption in the bandpass. The user selects the reference pixels and assigns them a mean reflectance value for the selected channels. A 2-dimensional LUT relating the visible range reciprocal to the pixel radiance and the spatially averaged radiance is then constructed. A surface plot of a typical LUT is shown in Figure 1. The visible range is reported for each reference pixel by interpolating from the LUT.

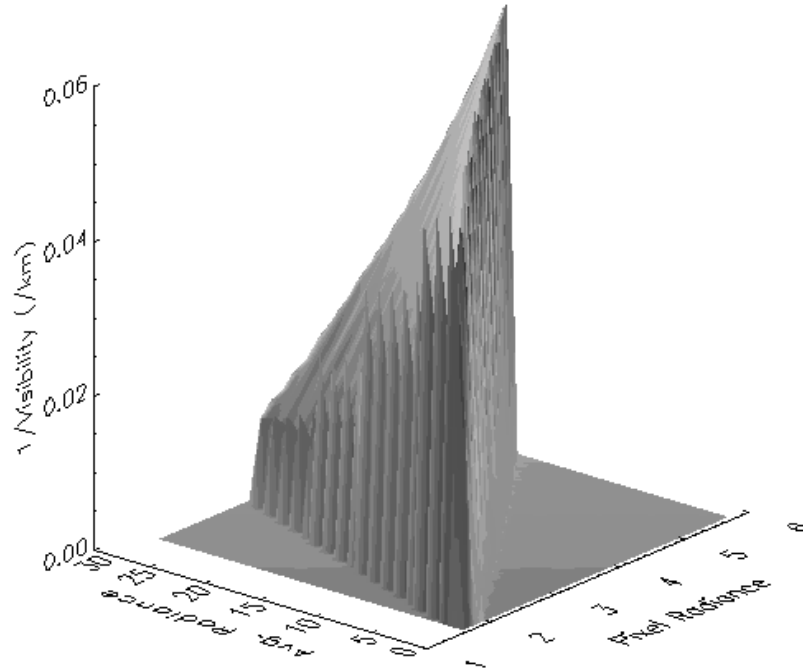


Figure 1. Look-up table for visible range determination. Right-hand axis is the pixel radiance in $\mu\text{W}/\text{cm}^2/\text{sr}/\text{nm}$, left-hand axis is the spatially averaged radiance in the same units and vertical axis is the reciprocal of the visible range in km^{-1} .

It should be noted that values taken from the diagonal of the table (averaged radiance = pixel radiance) correspond to neglect of the adjacency effect. When the reference pixels are taken from small areas in an image, such as calibration panels, isolated patches of vegetation, or shadows, the adjacency effect correction becomes critical. This is illustrated in Figure 2, which plots results from an analysis of spectral images of dark gray calibration panels in a grassy field. Visible ranges were retrieved from the panel spectra at two different wavelengths; MODTRAN's urban aerosol model was selected for the analysis. Values ranging from 20 to 100 km were retrieved when the adjacency effect was ignored; inclusion of the adjacency correction narrowed the range of results to between 20 and 25 km. Other similar analyses that we have performed to date suggest that a similar precision (i.e., around 0.01 km^{-1} for the reciprocal of the visible range) may be generally expected when using dark pixels and a realistic aerosol model.

If there are no "known" surfaces in the image, an alternative method must be used. Kaufman *et al.*⁸ have recently shown that for typical "dark" terrain the shortwave reflectance values (at $0.66 \mu\text{m}$ and $0.49 \mu\text{m}$ in particular) can be estimated from the reflectance at $2.1 \mu\text{m}$ by using empirical ratios. The $2.1 \mu\text{m}$ reflectance can be retrieved from an initial retrieval with an estimated aerosol, as it is not very sensitive to the assumed aerosol amount. Recently we have developed a generalized, single-step implementation of the reflectance ratio method. Agreement with retrievals based on calibrated reflectance panels has been found to be reasonable (to within 0.02 km^{-1} reciprocal visible range).

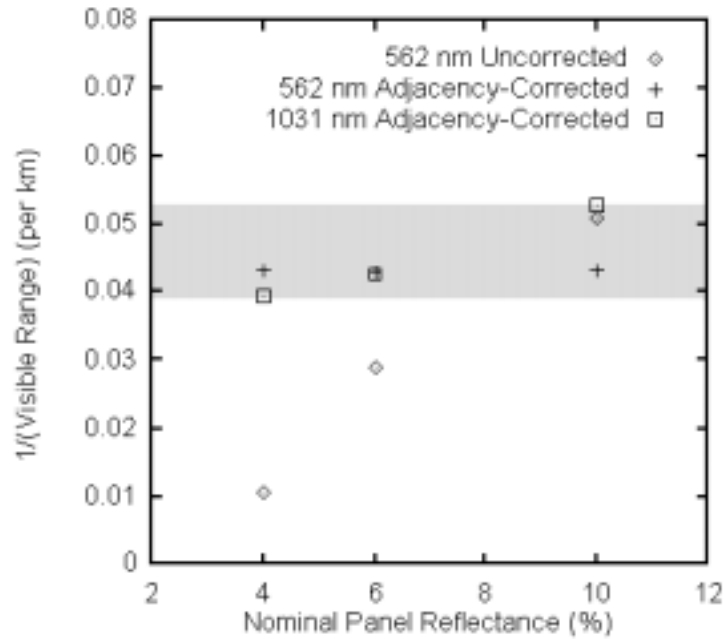


Figure 2. Visible ranges derived using pixels for three different gray calibration panels at two different wavelengths. No values were retrievable at 1031 nm without the adjacency correction. Shaded region shows the range of adjacency-corrected results.

4. RADIANCE DATA SIMULATION

A procedure has been developed for simulating radiance data cubes starting with a reflectance data cube and a water vapor column density map. To very briefly summarize the algorithm, the MODTRAN4 calculation described in Section 2 is performed for the desired sensing geometry and atmospheric model; the Equation (1) parameters are derived from the calculations; the reflectance is spatially averaged to generate ρ_c ; and the pixel radiances are calculated directly from Equation (1).

Sample results are shown in Figure 3. The original AVIRIS radiance image of the Moffett Field area (left) was atmospherically corrected using a visibility of 23 km with the MODTRAN rural aerosol model. The resulting surface reflectance data cube was inserted into the simulation algorithm to generate the same scene but with a 5-km visibility urban aerosol (right).



Figure 3. AVIRIS Moffett Field scene (left) and simulation with a 5 km visibility urban aerosol (right).

As a test of the numerical accuracy, we have performed reflectance retrievals on simulated data cubes using the same model atmosphere and viewing geometry assumed for the simulation. The results are very close to the original reflectances, although typically not in precise agreement because the averaged reflectance ρ_e used in the retrieval has not been converged. With no adjacency corrections in either the retrieval or simulation directions the original reflectances are reproduced very precisely (to within 0.001 outside extremely strong atmospheric absorption regions).

5. SPECTRAL POLISHING ALGORITHM

"Polishing" is a term coined by Boardman⁹ to describe a mathematical renormalization method for removing artifacts from reflectance spectra using only the data itself. When properly implemented, polishing dramatically reduces spurious, systematic spectral structure due to wavelength registration errors and molecular absorption residuals while leaving true spectral features of the surface intact. However, polishing cannot compensate for broad spectral shape errors caused by sensor gain miscalibration or uncompensated adjacency effects, for example.

The basic assumptions of polishing are: (1) spectral reflectance artifacts can be effectively removed by applying a spatially independent linear transformation (i.e., channel-dependent offsets and gain factors) to the spectra; (2) spectrally smooth "reference" pixels (for example, soil or pavement) can be found within the scene from which the transformation can be derived; (3) the true spectra of the reference pixels can be approximated by applying a smoothing operation. The offset and gain factors can be generated from the reference pixels by performing a linear regression fit of the smoothed spectra to the original spectra. If the offset is negligible, the gain factor can be obtained from ratios of the smoothed to original spectra.

Boardman's spectral smoothing method is based on a Legendre polynomial fit. An alternative polishing algorithm has been developed by Gao *et al.*¹⁰ in which the offset is ignored and the smoothing is accomplished with cubic spline fitting. We have developed a related, automated polishing method for our own atmospheric correction algorithm. The smoothing is performed by taking a running average over n adjacent spectral channels. Spectrum endpoint and missing-channel complications are limited if only a modest amount of smoothing is desired (n is low). For example, a lower- n smoothing is useful for removing residual sawtooth "noise" caused by a dark current offset between odd-numbered and even-numbered channels in some older AVIRIS data. A higher- n smoothing ($5 \leq n \leq 9$) is better for removing larger-scale artifacts such as atmospheric absorption band residuals.

There are many possible methods for selecting the reference pixels from which the linear transformation is generated. In our current algorithm the normalized variance between the smoothed and unsmoothed pixels is calculated and histogrammed and all pixels whose values lie below the peak of the histogram are selected. The gain factor is taken as the ratio of the RMS smoothed to RMS unsmoothed spectrum for these pixels. Compared with Gao *et al.*'s method of averaging individual smoothed to unsmoothed spectrum ratios, our method of calculating the gain factor more heavily weights high reflectance values, which are proportionally less affected by any offset and may be less likely to contain true absorption features that should not be removed by the polishing.

An example of the effect of polishing is shown in Figure 4 for a retrieved spectrum of a calibration panel. The advantage of spectral polishing over simple smoothing is evident, as true, sharp absorption features of the panel's vinyl overlay at 674 nm and 1712 nm are preserved while equally sharp artifacts elsewhere in the spectrum are eliminated or reduced. While the success of spectral polishing and other renormalization methods is already considerable, we believe that these methods will continue to improve as they become more fully developed.

6. VALIDATION OF REFLECTANCE SPECTRUM RETRIEVALS

Validation is ideally achieved via comparisons with simultaneously measured "ground truth" reference surfaces. Validations with AVIRIS data have been conducted primarily with large, uniform natural surfaces such as dry lake beds measured in clear, dry weather. These conditions do not however test the ability of the correction algorithm to handle strong molecular absorption and aerosol effects. An alternative is to use smaller, readily characterized surfaces such as calibration panels; these measurements can be conducted in a variety of locations and weather conditions, but they require a sensor with a small footprint. With small surfaces and moderate to high aerosol levels, the adjacency effect becomes important and needs to be corrected. An example is given in Figure 5. The adjacency effect, which is not corrected in the ATREM⁵ retrieval shown, appears as a superposition of an average background spectrum, consisting mainly of grass and trees, on the panel spectra at short wavelengths (note the sharp chlorophyll edge around 700 nm). The chlorophyll edge is absent in the spectra retrieved

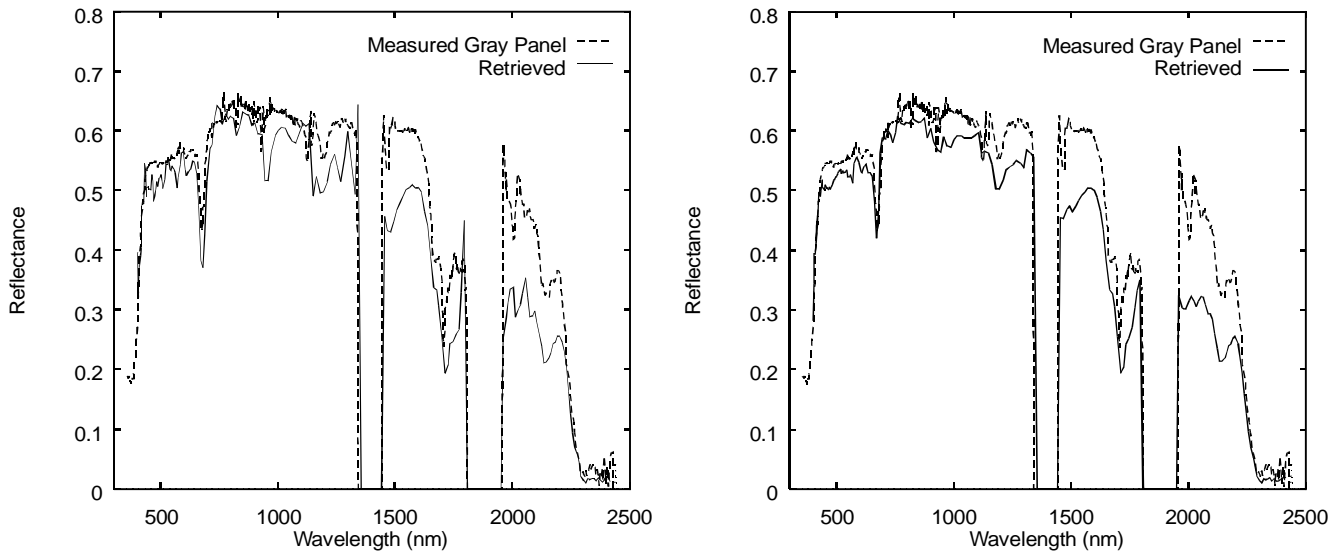


Figure 4. Retrieved reflectance spectrum of a nominal 64% gray calibration panel before (left) and after (right) polishing.

with the current algorithm and the visible portions are reasonably flat, consistent with the "ground truth" data. However, some molecular absorption residuals remain and there is evidence for sensor calibration errors, especially at the longer wavelengths.

Even when "ground truth" measurements are not available, the success of the correction for atmospheric absorption bands can be assessed from spectra of objects or terrain that are known to be spectrally smooth and thus highlight any absorption band residuals. Different atmospheric correction algorithms tend to yield similar, good results under clear, dry, high-sun conditions; an example is shown in Figure 6. On the other hand, we find large absorption residuals when analyzing data taken in a moist atmosphere (Figure 7); similar results are expected with a high water column along the sun-surface-sensor path due to a low sun. With ATREM the residual problems are more pronounced and the retrieved water amounts seem too large. With the current MODTRAN4-based algorithm the main problem is that a higher column density is required to correct (and is therefore retrieved from) the 0.94 μm band compared to the 1.13 μm or longer wavelength bands, the fractional error increasing with the water column. When retrieving water with the 1.13 μm band a residual 0.94 μm absorption band appears in the reflectance spectrum, as shown in Figure 7 and to a lesser extent in Figure 5. Conversely, when retrieving at 0.94 μm the reflectance shows a spike at 1.13 μm as well as at the longer wavelength water band edges. For the Figure 7 data the column water vapor retrieved from the 0.94 μm band exceeds that retrieved from the 1.13 μm band by 40%.

Several factors may contribute to this poor behavior of the atmospheric correction at high water columns. One is approximations in modeling the coupling of molecular absorption and atmospheric scattering. For example, we have found that the water absorption depths are somewhat sensitive to the choice of multiple scattering algorithm (DISORT 8-stream versus Isaacs 2-stream) in MODTRAN4 and also to whether the more accurate but time-consuming correlated- k option is used. However, independent evidence suggests that the major problem is with short wavelength water vapor spectroscopy rather than the handling of scattering. For example, we have found 0.94 μm versus 1.13 μm absorption inconsistencies of a similar size when using MODTRAN4 to model a ground-based radiance measurement, conducted at the DOE ARM site in Oklahoma, of a direct sun-illuminated Spectralon panel from which the skylight component had been subtracted. The MODTRAN4 analysis of the panel measurements only requires calculation of transmitted solar irradiance and does not involve use of a scattering algorithm. We also observe excess 0.94 μm absorption in AVIRIS data taken under extremely clear conditions (around 100 km visible range). Finally, these findings are consistent with a report by Halthore *et al.*¹¹ of excessive water vapor retrieved from 0.94 μm measurements compared to microwave radiometer data.

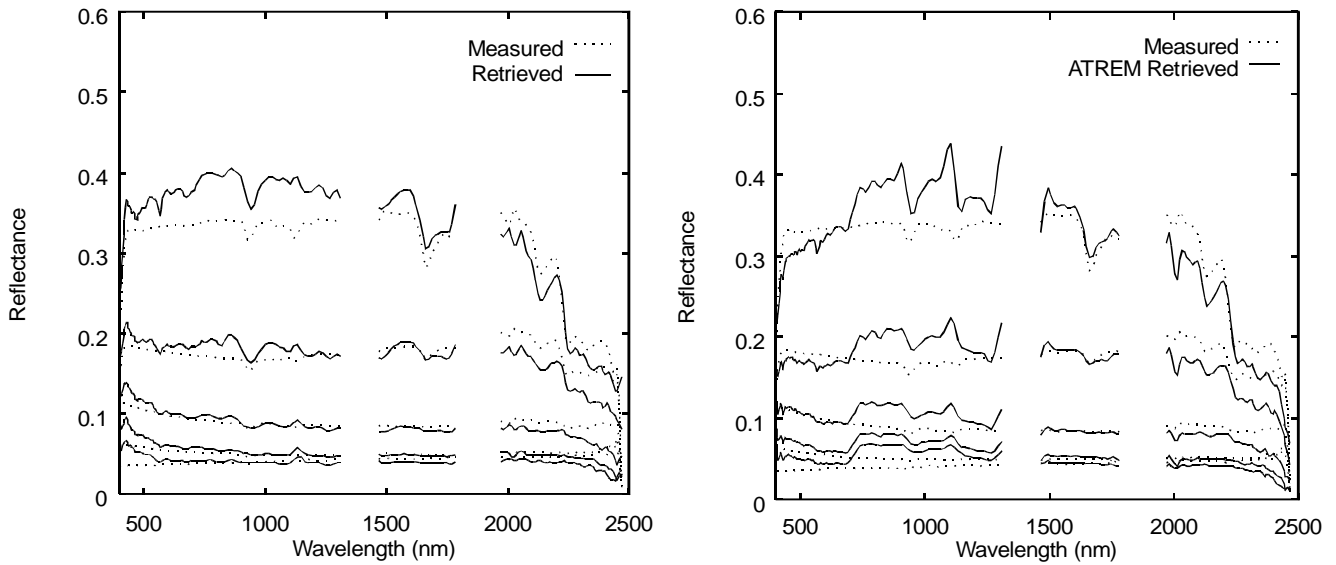


Figure 5. Comparison of "ground truth" measurements of calibration panels with spectra retrieved using the current atmospheric correction algorithm (left) and ATREM (right). The retrieved spectra have been smoothed slightly but not polished.

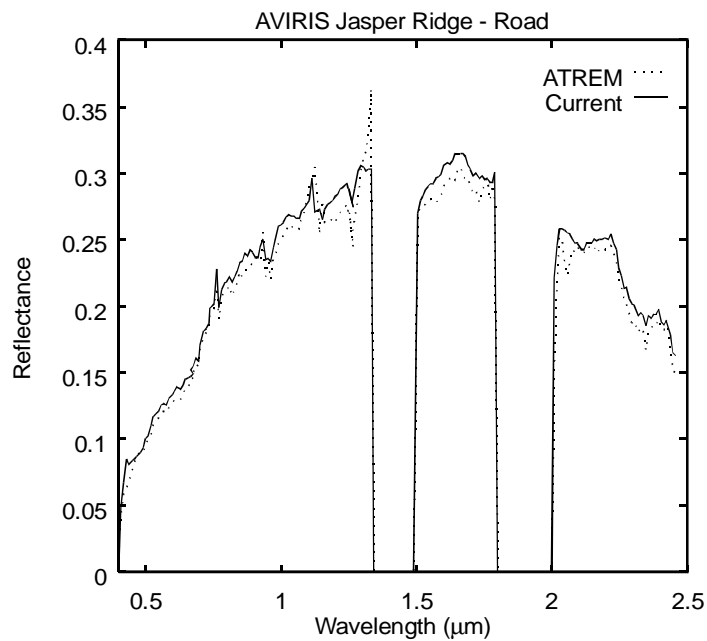


Figure 6. AVIRIS spectrum of a paved highway retrieved from 4/3/97 Jasper Ridge data using the current algorithm (solid line) and ATREM (dashed line). No polishing, smoothing, or adjacency correction were used. The retrieved column water vapors are respectively 0.72 cm (from the 1.13 μm band) and 0.75 cm (average from 0.94 and 1.13 μm bands) with the two codes.

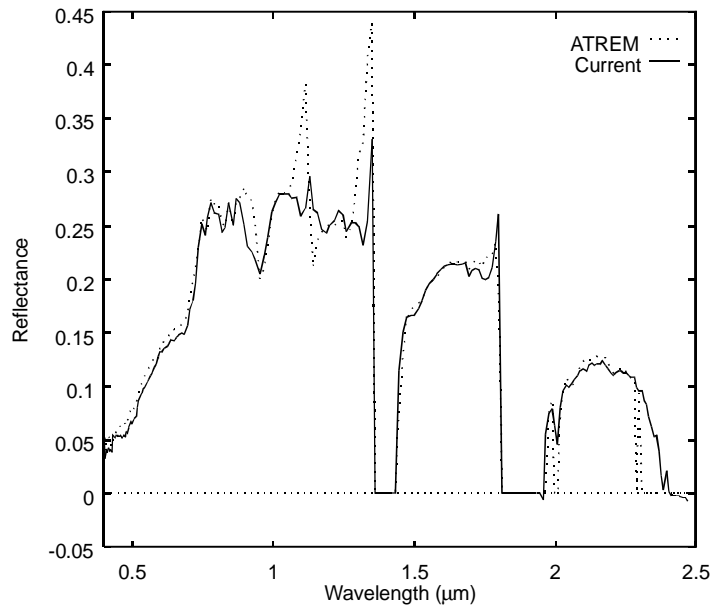


Figure 7. Retrieved spectra of a dirt road from measurements of a forested scene at Keystone, PA. No adjacency correction, spectral smoothing or polishing were used. The retrieved visible range is 15 km; the retrieved column water vapor is 3.4 cm from the current algorithm (1.13 μm band) and 6.1 cm from ATREM (average from 0.94 and 1.13 μm bands).

Since the line strengths for the 0.94 μm and 1.13 μm bands both appear to be well established experimentally (references to recent measurements are given in the HITRAN database¹²) and the water column inconsistency is a function of the column amount, we conjecture that the problem lies in the water continuum component. The continuum has never been directly measured for the 0.94 μm band; the model used in MODTRAN4 is an extrapolation based on mid-wave IR measurements.¹³ The continuum accounts for an increasing proportion of the net absorbance with increasing water column amounts because its curve of growth follows Beer's law rather than the square-root law of the line spectrum. Under the conditions of the measurements mentioned above, the presence of the continuum has a tens-of-percent effect on the retrieved column amount. This explains why ATREM, which omits the continuum entirely, often retrieves unrealistically high water amounts in moist atmospheres (e.g., in Figure 7).

Atmospheric absorption residuals for two species besides water have also been identified in retrieved reflectance spectra. One is associated with the CO_2 bands near 2 μm ; a residual structured absorption on the order of 10% of the reflectance often appears here. A similar problem occurs with ATREM. Based on "exact" line-by-line transmittance calculations the problem appears to be due to inaccuracies in the absorption band models. Another is a small (<10%) residual O_2 absorption at 1.27 μm ; this is caused by omission of a collision-induced continuum component. MODTRAN4 will soon be upgraded to include this and other atmospherically important collision-induced spectral features.¹⁴

ACKNOWLEDGEMENTS

The work at Spectral Sciences was supported by the USAF contract no. F19628-91-C-0145 and by the Lincoln Laboratory purchase order BX-6926 under USAF contract no. F19628-95-C-002.

REFERENCES

1. A. Berk, L.S. Bernstein, G.P. Anderson, P.K. Acharya, D.C. Robertson, J.H. Chetwynd and S.M. Adler-Golden, "MODTRAN Cloud and Multiple Scattering Upgrades with Application to AVIRIS," *Remote Sens. Environ.*, Vol. 65, pp. 367-375, 1998.
2. K. Staenz, D.J. Williams and B. Walker, "Surface Reflectance Retrieval from AVIRIS Data Using a Six-Dimensional Look-Up Table," *Summaries of the Sixth Annual JPL Airborne Earth Science Workshop*, March 4-8, 1996, JPL Publication 96-4, Vol. 1, Pasadena, California, pp. 223-229, 1996.

3. E.F. Vermote, N. El Saleous, C.O. Justice, Y.J. Kaufman, J.L. Privette, L. Remer, J.C. Roger and D. Tanre, "Atmospheric Correction of Visible to Middle-Infrared EOS-MODIS Data Over Land Surfaces: Background, Operational Algorithm and Validation," *J. Geophys. Res.*, Vol. 102, pp. 17131-17141, 1997.
4. D.J. Williams, A. Royer, N.T. O'Neill, S. Achal and G. Weale, "Reflectance Extraction from CASI Spectra Using Radiative Transfer Simulations and a Rooftop Radiance Collector," *Can. Journal of Remote Sensing*, Vol. 18, pp. 251-261, 1992.
5. B.-C. Gao, K.B. Heidebrecht and A.F.H. Goetz, *Atmosphere Removal Program (ATREM) Version 2.0 Users Guide*, Center for the Study of Earth from Space/CIRES, University of Colorado, Boulder, Colorado, 26 pages, 1996.
6. R. Richter, "Atmospheric Correction of DAIS Hyperspectral Image Data," *SPIE AEROSENSE '96 Conference*, Orlando, FL, April 8-12, SPIE Proceedings, Vol. 2758, 1996.
7. E. Vermote, D. Tanre, J.L. Deuze, M. Herman and J.J. Morcrette, *Second Simulation of the Satellite Signal in the Solar Spectrum (6S)*, 6S User Guide Version 6.0, NASA-GSFC, Greenbelt, Maryland, 134 pages, 1994.
8. Y.J. Kaufman, A.E. Wald, L.A. Remer, B.-C. Gao, R.-R. Li and L. Flynn, "The MODIS 2.1- μ m Channel--Correlation with Visible Reflectance for Use in Remote Sensing of Aerosol," *IEEE Transactions on Geoscience and Remote Sensing*, Vol. 35, pp. 1286-1298, 1997.
9. J.W. Boardman, "Post-ATREM Polishing of AVIRIS Apparent Reflectance Data using EFFORT: a Lesson in Accuracy versus Precision," *Summaries of the Seventh JPL Airborne Earth Science Workshop*, JPL Publication 97-21, Vol. 1, p. 53, 1998.
10. B.-C. Gao, M. Liu and C.O. Davis, "A New and Fast Method for Smoothing Spectral Imaging Data," *Summaries of the Seventh JPL Airborne Earth Science Workshop*, JPL Publication 97-21, Vol. 1, pp. 131-140, 1998.
11. R.N. Halthore, T.F. Eck, B.N. Holben and B.L. Markham, "Sun Photometric Measurements of Atmospheric Water Vapor Column Abundance in the 940-nm Band," *J. Geophys. Res.*, Vol. 102, pp. 4343-4352, 1997.
12. L.S. Rothman, C.P. Rinsland, A. Goldman, S.T. Massie, D.P. Edwards, J.-M. Flaud, A. Perrin, C. Camy-Peyret, V. Dana, J.-Y. Mandin, J. Schroeder, A. McCann, R.R. Gamache, R.B. Wattson, K. Yoshino, K.V. Chance, K.W. Jucks, L.R. Brown, V. Nemtchinov and P. Varanasi, "The HITRAN Molecular Spectroscopic Database and HAWKS (HITRAN Atmospheric Workstation): 1996 Edition," *J. Quant. Spectrosc. Radiat. Transfer*, Vol. 60, pp. 665-710, 1998.
13. S.A. Clough, F.X. Kneizys and R.W. Davies, "Line Shape and the Water Vapor Continuum," *Atmospheric Research*, Vol. 23, pp. 229-241, 1989.
14. Solomon, S., R.W. Portmann, R.W. Sanders and J.S. Daniel, "Absorption of Solar Radiation by Water Vapor, Oxygen and Related Collision Pairs in the Earth's Atmosphere," *J. Geophys. Res.*, Vol. 103, pp. 3847-3858. 1998